

# A98-31707

ICAS-98-7,6,1

## AIRCRAFT LOAD MODELS FOR A PILATUS PC-9 BASED ON WIND TUNNEL TESTING

Anthony Huang

The Sir Lawrence Wackett Centre for Aerospace Design Technology  
Royal Melbourne Institute of Technology  
GPO Box 2476V, Melbourne, VIC 3001, AUSTRALIA

### Abstract

Aircraft load models for a Pilatus PC-9 based on wind tunnel testing have been developed to determine flight loads including shear, bending, and torque on the lifting surfaces in both trimmed and untrimmed longitudinal flight. Experimental results generated by the load models represent realistic flight conditions in untrimmed longitudinal flight. However, load distributions obtained for trimmed level flight are inaccurate, as the models have not yet been capable of providing accurate predictions for the angle of attack and elevator deflection required in trimmed flight due to insufficient information on aircraft aerodynamic characteristics. An independent aerodynamic model based on lifting line theory has been developed to act as a tool for estimating flight loads. Results predicted by theory involve apparent errors, particularly for the tail, and the errors are mainly due to inadequate accuracy or detail of the geometry modelled. As there is still a room for improvement of results to be made, further modifications on the load models should be necessary to obtain more accurate values for flight loads.

### Nomenclature

$a$	lift-curve slope
$a_1$	tail lift-curve slope
$a_2$	elevator lift-curve slope
$\Delta A$	area of a discrete panel
$c$	chord
$C_d$	drag coefficient (2-D)
$C_l$	lift coefficient (2-D)
$C_m$	pitching-moment coefficient
$C_{m_0}$	pitching-moment coefficient at zero airplane lift
$C_{m_{owb}}$	wing-body pitching-moment coefficient at zero wing-body lift
$C_p$	pressure coefficient
$C_{pL}$	lower surface pressure coefficient
$C_{pU}$	upper surface pressure coefficient
$h_0$	neutral point of airplane, fraction of mean chord
$s$	semispan
$V$	airspeed (equivalent)
$x$	a lifting surface chordwise station measured from surface leading edge
$y$	a lifting surface spanwise station measured from aircraft centreline
$\alpha$	surface incidence

$\eta$	elevator deflection
$\varepsilon$	downwash angle
$\rho$	air density

### Abbreviations

2-D	two-dimensional
3-D	three-dimensional
AMRL	Aeronautical and Maritime Research Laboratory
AOA	angle of attack
DSTO	Defence Science and Technology Organisation
RMIT	Royal Melbourne Institute of Technology

### 1. Introduction

This research is part of Royal Melbourne Institute of Technology (RMIT) / Defence Science and Technology Organisation (DSTO) Centre of Expertise in Aerodynamic Loading project. The ultimate aim of the joint project is to access the fatigue life of various fighter aircraft used in Australia. Determination of aerodynamic load distributions on aircraft lifting surfaces during flight is essential if aircraft fatigue properties are to be analysed. The loading is intended to be representative of the actual service usage of the aircraft by the Royal Australian Air Force<sup>(1)</sup>.

The objective of this research is to develop load models and analyze flight loads on PC-9 aircraft lifting surfaces in longitudinal flight. The analysis is based on experimental data obtained from Aeronautical and Maritime Research Laboratory (AMRL) wind tunnel testing. An independent aerodynamic model of the PC-9 using the lifting line method has been developed as a tool for comparing experimental results. Flight loads generated by these load models will be compared with those measured during flight test and those calculated using computational fluid dynamics analysis, so that discrepancies of results using different methods can be observed. Once the flight loads are known, they can be used in fatigue testing.

The PC-9 is already undergoing fatigue testing with assumed, but perhaps incorrect flight loads. The results of this work will be used to verify the values of loads employed in the testing and to help define loads for British Aerospace Hawk.

2. Development of an Independent Aerodynamic Model of PC-9 using Lifting Line Method

Lifting line theory is based on finite wing aerodynamics. It basically models wing lift, drag, and spanwise lift distribution. The equations involved for solving these aerodynamic characteristics can be found in References [2, 3 & 4]. The lifting surface local lift coefficients predicted by lifting line theory were used as the source for determining the pressure coefficients. These pressure coefficients were then further developed to form shear, bending, and torque. An aerodynamic model of PC-9 has been developed using PASCAL programming language. The development of the model is discussed in more detail in the following subsections.

2.1 Aerofoil Aerodynamic Analysis

The full-scaled PC-9 wing is made of PIL15M825/PIL23M850 (root/tip) aerofoil sections. However, the wing section employed in this independent aerodynamic model is based on NACA4312 aerofoil and the tailplane developed is based on NACA0009 aerofoil to simplify the geometry input for analysis. It is assumed that NACA4312 and NACA0009 have very similar aerodynamic characteristics as the original aerofoil sections of the wing and tailplane respectively.

The two-dimensional (2-D) aerodynamic performance of the lifting surfaces was analysed using the EPPLER\* program. After the geometry of the airfoil section, Reynolds number, compressibility option, boundary layer transition option, and angles of attack (AOAs) were defined, the aerofoil  $C_l$ ,  $C_d$  and  $C_m$  with respect to  $\alpha$  (&  $\eta$ ) and chordwise  $C_p$  distribution were generated. The aerofoil aerodynamic characteristics obtained for both wing and tailplane will be needed in the later stages of PC-9 model development.

2.2 Lifting Line Calculations

Before lifting line calculations are carried out, the geometry of the model as described in References [5 & 6] needs to be defined. The full scale model is employed throughout the entire research. In developing the wing, the dihedral angle of 7° was ignored, since lifting line method is unable to model this tilting angle. It is assumed that the ignorance of this dihedral angle would not affect results significantly. With the basic geometry established, the calculations using lifting line method were performed.

Two-dimensional lift-curve slopes for both wing and tailplane sections have been obtained by using EPPLER program. These slopes were converted into three-dimensional values based on lifting line method. For each angle of attack input, the preliminary lifting line program

developed generates a 3-D lift coefficient. It was found that the 3-D value of lift-curve slope for the wing with consideration of fuselage effect, 3.87/rad, is significantly smaller than the 2-D value, 5.97/rad.

Determination of the tailplane lift-curve slopes was found more complicated, as it involved an additional angle contributed by the elevator. The interference effects from the wing does not need to be considered here. The wing interference as a downward deflection of the flow at the tail is characterized by the downwash angle  $\epsilon$ , and it is treated as a change in incidence at the tail.

The lifting line method cannot model the elevator effect directly from the elevator angle, so that the angle is replaced by an equivalent change of the tailplane angle, as described by equation (1). With a positive elevator (or flap) deflection, there is an increase in lift and sometimes a change in lift-curve slope.

$$\alpha_{eff} = (\alpha_{eff})_{noflap} + \Delta\alpha_{flap} \dots\dots\dots (1)$$

$$\text{where } \Delta\alpha_{flap} = \frac{(\Delta C_L)_{flap}}{a_{flap}}$$

It was found that the 3-D  $a_1$  is 4.0/rad, and the 3-D  $a_2$  is 3.27/rad.

2.3 Development of Lifting Surface Pressure Distributions

The pressure distributions over lifting surfaces were developed based on results obtained from lifting line calculations and sectional performance. The local lift coefficients along the span of the lifting surfaces were used as the source for determining the pressure coefficients. These local lift coefficients generated by lifting line theory were treated the same as the 2-D lift coefficients for an aerofoil section. For a given  $C_l$  and aerofoil section, an equivalent 2-D  $\alpha$  was determined by using EPPLER program. After the  $\alpha$  was obtained, the aerofoil program was then used to generate the pressure distribution or a set of  $C_p$  at points defining the aerofoil section. It was found that there is a close to linear correlation between  $C_p$  and  $C_l$ .

Since 20 spanwise stations or 20 local  $C_l$  were employed for each semispan of the wing and tailplane, it would be extremely inefficient and time consuming to model the pressure distributions at all stations manually. Hence, a data-interpolation program was developed to calculate the equivalent  $C_p$  at each discrete chordwise points on top and bottom surfaces of the section for a given  $C_l$ . The entire pressure distribution over a lifting surface was obtained by running the program 20 times for 20 different  $C_l$  at 20 spanwise stations.

\* By Dr. Richard Eppler

### 2.4 Development of Lifting Surface Shear, Bending, and Torque Distributions

The final stage in the development of the aerodynamic model of PC-9 involved converting pressure coefficients over lifting surfaces into shear, bending, and torque. The sign convention for pressure is positive acting towards the lifting surface. Thus, the pressure acting upward is negative on the upper surface and positive on the lower surface.

The shear force is the summation of normal forces acting at discrete panels over the lifting surface, as described by equation (2). The sign convention for the shear is positive upward.

$$Shear = -\frac{1}{2} \rho V^2 \left[ \sum C_{pu} \Delta A - \sum C_{pl} \Delta A \right] \quad (2)$$

where  $\Delta A$  = area of discrete panels

The bending moment at a distance  $y_1$  from the centerline (longitudinal axis) of the aircraft is given by equation (3). It is positive for surface tip bending upward.

$$BM = \frac{1}{2} \rho V^2 \left\{ \int_{y_1} \left[ - \left( \int C_{pu} dx \right) \cdot (y - y_1) \right] dy + \int_{y_1} \left[ \left( \int C_{pl} dx \right) \cdot (y - y_1) \right] dy \right\} \quad (3)$$

where  $y$  = a lifting surface spanwise station  
 $s$  = semispan  
 $c$  = local chord length  
 $dx$  = chordwise length of a discrete panel  
 $dy$  = spanwise length of a discrete panel

The torque about a reference point on the lifting surface is given by equation (4). It is positive for surface trailing edge down.

$$Torque = \frac{1}{2} \rho V^2 \left\{ \int_{y_1} \left[ \int C_{pu} \cdot (x - x_{ref}) dx - \int C_{pl} \cdot (x - x_{ref}) dx \right] dy \right\} \quad (4)$$

where  $x_{ref} = 0.5$  for wing (quarter chord)  
 $= 0.7$  for tailplane (hinge line)

### 2.5 Trimmed Flight

An aircraft is said to be trimmed if it is in level flight while maintaining a constant angle of attack. For this condition to be satisfied, the lift generated on the aircraft must be equal to its weight and the pitching moment must

be zero. For the analysis contained in this paper, aeroelastic effects and moments due to thrust and drag are ignored. Hence the analysis applies to a rigid airplane in gliding flight.

### 3. Development of PC-9 Load Models based on Experimental Data

The PC-9 load models have been developed based on wind tunnel testing conducted by AMRL. The experimental raw data are in the form of local pressure coefficients. The tasks involved in the development of the models included filtering and arranging data and converting them into flight loads. The models developed are meant for determining flight loads on lifting surfaces for a given airspeed, angle of attack, and elevator deflection. For trimmed flight, these angles required are calculated using the trim equations. The aerodynamic parameters in the equations are determined from wind tunnel test data.

The experimental raw data including local pressure coefficients, geometry specification including the panel area, panel coordinates in Global Reference Frame, and panel unit normal, are initially presented in hundreds of files for different combinations of AOA, angle of sideslip, elevator, rudder, and aileron deflections, and propeller setting. The data for AOA =  $-4^\circ$ ,  $2^\circ$ ,  $8^\circ$  and  $14^\circ$  and  $\eta = -15^\circ$ ,  $-5^\circ$ ,  $0^\circ$  and  $10^\circ$  with no prop setting and  $V = 60$  m/s were chosen for initial analysis. Since the investigation is for longitudinal flight without any lateral motion, the data for zero sideslip and zero rudder and aileron deflections were the only interest.

The initial work involved filtering the pressure data, so that only the data on starboard lifting surfaces were analysed. The analysis was simplified by reducing the data size, and this was valid because of symmetrical loading about the aircraft longitudinal axis in longitudinal flight. After eliminating insignificant data, the next step was to sort the data. The data were arranged so that their panel numbers were in ascending order. The geometry specification was then identified and extracted for each panel.

For cases that the AOA and elevator deflection are arbitrarily chosen and the pressure data for these angles are not available, data interpolation needs to be applied. The data interpolation program described earlier was further developed to calculate equivalent  $C_p$  for a given AOA and  $\eta$  across all the panels. The calculations are based on the data sets for the four AOAs and  $\eta$  selected, and hence the angle of attack and elevator deflection chosen for analysis must be within the range of  $-4^\circ \sim 14^\circ$  and  $-15^\circ \sim 10^\circ$  respectively.

With the basic pressure and geometry data established, the next step was to divide the data into two

separate sets for upper and lower surfaces of the wing or tail. Data for upper and lower surfaces were distinguished based on the sign of unit normal in z direction. Positive sign of unit normal in z direction denotes upper surface and negative denotes lower surface. There are 376 and 384 measurements on wing upper and lower surfaces respectively and 163 and 147 measurements on tailplane upper and lower surfaces respectively. Following the step, data sets were further refined by eliminating some unwanted data, such as the data for the joints between the tailplane and the fuselage rear section, and arranging data so that the data on the same spanwise section are put together and in the appropriate order.

The final stage in the development of load models involved converting pressure coefficients into flight loads in the form of shear, bending, and torque. Equations (2) ~ (4) with some modifications were employed, as the experimental data involve an additional parameter of unit normal and different reference points.

#### 4. Results and Discussion

Results for flight loads on PC-9 lifting surfaces have been obtained based on wind tunnel tests and theory. The independent aerodynamic model based on lifting line method is meant for predicting flight loads with certain accuracy. The results determined from wind tunnel testing data represent measured aerodynamic loads, but still comprise some experimental errors. The independent aerodynamic model can be used for further analysis only if the results generated by the model compare well with experimental results.

##### 4.1 Untrimmed Longitudinal Flight

As flight loads comprising shear, bending, and torque were determined from results of pressure distributions, comparisons of theoretical and experimental pressure distributions need to be made. With reference to Figure 1 & 2, it can be observed that at zero AOA the pressure distributions on the upper surface of the wing using the two methods are quite similar. However, the pressure distributions on the lower surface portray obvious discrepancies in chordwise direction. The experimental result shows that the nose has the largest  $C_p$  on the surface that is positive, while the result predicted by theory indicates negative or minimum  $C_p$  at the section.

When comparisons of pressure distributions on the tail using the two methods are made, with reference to Figure 3 & 4, it can be seen that there are some discrepancies at zero incidence and zero elevator deflection, particularly near both leading edge and trailing edge. Over both upper and lower surfaces, the experimental results show smooth distributions at the trailing edge, while the theoretical results show an increase in  $C_p$  there. At the leading edge of the lower surface,

theory predicts an increase in pressure while the experimental result shows a decrease there. The distinct trends of pressure distributions using the two methods, particularly in the chordwise direction, have the direct effect on the results of torque.

The wind tunnel and theoretical results plotted in Figure 5a shows the comparison of shear distributions on the wing at zero AOA. Generally the theory predicts higher shear and the load is approximately 500 N above the experimental value throughout most of the wing. When AOA is increased to  $8^\circ$ , the comparison as presented in Figure 5b shows that there is an improvement in agreement between prediction and measurement if the discrepancy is considered in term of percentage error. However, the actual magnitudes indicate that 550 N of difference in shear still remains at the root, and the prediction becomes lower than measurement. The discrepancy of the results may be due to inaccurate modelling of the wing section, incompetence of the theory for modelling wing dihedral, and possibly experimental errors in wind tunnel testing.

Figure 6a shows the comparison between theoretical and experimental results for bending moment over the wing at zero AOA. Since bending moment is dependent upon shear, the result from the lifting line theory for bending is also greater than the result obtained from experiment. The variance of results increases from zero at the tip to a maximum value of approximately 2600 N.m at the root. Similar trends of results are presented when the AOA is increased to  $8^\circ$ , as illustrated in Figure 6b.

Integrated results for wing torque at zero AOA from wind tunnel tests and theory are presented in Figure 7a. The Figure indicates that the magnitude of torque (in pitch-down direction) predicted by theory is lower than the wind tunnel result at this angle. As AOA is increased to  $8^\circ$ , the experimental result becomes the one with larger magnitude and the difference of results becomes significant on the outer surface, as shown in Figure 7b. The discrepancy may be due to either inaccurate modelling of the wing section by theory or experimental errors.

Figure 8a shows the comparison of experimental and theoretical shear distributions over the tailplane at AOA =  $0^\circ$  &  $\eta = 0^\circ$ . Generally the theory based on lifting line method underestimates the shear in downwards direction, and the magnitude at the root is approximately half of the value from wind tunnel tests only. The theoretical location of tailplane tip shown in the figure is outboard the experimental one because the mass balance outboard the tailplane section is included as well in predictions. The results for AOA =  $8^\circ$  &  $\eta = -5^\circ$  illustrated in Figure 8b shows very similar trends of comparisons. Since the difference of results for the tail is much more obvious than for the wing, it is believed that the significant

discrepancies of results are more likely to be due to inaccurate modelling the tailplane by theory than experimental errors. It was found that the tailplane section employed in the independent aerodynamic model has significantly different aerodynamic characteristics from the actual section used in the tests.

Figure 9a shows the comparison of bending moments integrated from the two methods for the tailplane at  $AOA = 0^\circ$  &  $\eta = 0^\circ$ . Since the bending moment is dependent on shear, the theory again underestimates the result in downwards direction. Significant discrepancy also occurs. Similar trends of results for  $AOA = 8^\circ$  &  $\eta = -5^\circ$  are presented in Figure 9b.

Figure 10a shows the comparison of torque for the tailplane at  $AOA = 0^\circ$  &  $\eta = 0^\circ$  using the two methods. The figure indicates severe discrepancies between theoretical and experimental results again. The results for  $AOA = 8^\circ$  &  $\eta = -5^\circ$  illustrated in Figure 10b show similar trends of comparisons. The torque predicted by the theory is significantly lower in magnitude than the experimental value.

#### 4.2 Trimmed Level Flight

For trimmed flight, the agreement between experimental and theoretical results not only depends on how accurate the independent aerodynamic model predicts flight loads for a given AOA and elevator deflection, but also depends on how well these angles for trim flight from the two methods compare with each other. The table below presents comparisons of AOAs and elevator deflections for trimmed flight determined from the two methods.

		V= 50 m/s	V= 100 m/s	V= 150 m/s
Experimental	AOA	9.03°	0.09°	-1.57°
	$\eta$	-7.11°	1.21°	2.75°
Theoretical	AOA	8.70°	-0.73°	-2.47°
	$\eta$	-2.45°	2.58°	3.51°

Comparisons illustrated show that there is a better agreement for the AOA than for the elevator deflection estimated from wind tunnel tests and theory generally. For the AOA, the difference of the results is generally within  $1.2^\circ$ , and the discrepancy becomes smaller as the airspeed increases. For the elevator deflection, the results generated show that the discrepancy becomes more significant as the airspeed is decreased, and the difference of the angles estimated can be up to  $6.3^\circ$  for  $V = 50$  m/s.

The errors comprised in the experimental results for these angles may be as significant as the errors for values predicted by theory or even larger, because of inaccurate values of  $h_o$  and  $Cm_{owb}$  used due to insufficient information provided. Thus, good agreement between theoretical and experimental values of AOA and elevator

deflection for trimmed flight does not necessarily present accurate estimations for these angles. For better agreement of results or more reliable results to be achieved, the accuracy of flight loads generated by the independent aerodynamic model and the accuracy of AOA and elevator deflection for trimmed flight from both methods needs to be improved.

#### 5. Conclusions and Recommendations

The PC-9 load models have been developed using experimental data from wind tunnel tests and theory based on lifting line method. They are used to determine flight loads including shear, bending, and torque on the aircraft wing and tailplane in longitudinal flight.

Experimental results derived from wind tunnel pressure measurements over the lifting surfaces represent simulate flight conditions. The load models generate realistic aerodynamic load distributions in untrimmed longitudinal flight (for a given AOA and elevator deflection). However, due to insufficient information and hence unrealistic  $Cm_{owb}$ ,  $h_o$ , and  $\epsilon$  assumed for the aircraft, the models have not been capable of providing accurate predictions for the AOA and elevator deflection required for a given speed in trimmed flight. Consequently, certain errors are involved in the aerodynamic loads generated for trimmed flight.

The independent aerodynamic model based on lifting line theory acts as a tool for estimating aircraft flight loads. The simplified wing and tailplane sections may be the most serious source of errors in the model, as geometry changes may constitute significant variation of lifting surface aerodynamic characteristics and hence load distributions. The incompetence of the theory for modelling wing dihedral may have some influences on the results as well. With the elevator deflection replaced by equivalent change of the tailplane angle in lifting line calculations, the accuracy of the results for tail loads has been degraded.

Comparisons of theoretical predictions with the integrated results from wind tunnel tests have been made for a number of test conditions. Based on the results of the two test cases studied, a reasonable correlation between theoretical analysis and experimental results was obtained for the wing in untrimmed longitudinal flight. However, the comparisons of the results for the tail demonstrated apparent underestimates of flight loads in magnitude from theory. Significant discrepancies of the results are mainly due to inaccurate modelling of the tailplane section and geometry by theory, as the experimental analysis portrays distinct tailplane aerodynamic characteristics from the performance of the tail employed in theory. Inaccurate modelling of the flow at the tail due to downwash effects may possibly be another source of theoretical errors. The airflow and geometry modelling needs to be very accurate

in order to produce good comparisons. Based on the results of the three test cases studied, the load distributions in trimmed flight obtained from the two methods appear to be a doubt as the comparisons of the results showed significant discrepancies. The accuracy of the required AOA and elevator deflection in trimmed flight determined are doubtful due to uncertain  $C_{m_{owb}}$  and  $h_o$  and varied lift-curve slopes and zero-lift incidences used in the two methods. As a result, the reliability of the predictions for aerodynamic load distributions in trimmed flight appears to be unsatisfactory.

Overall, the PC-9 load models based on wind tunnel testing provide valuable information on wind tunnel data handling process and aerodynamic load distributions over lifting surfaces. The independent model based on lifting line theory proves its usefulness as a preliminary design tool to estimate flight loads. To improve the predictions of results and to correctly describe flight loads in both trimmed and untrimmed longitudinal flight, further modifications should be necessary for more sophisticated models to be built, but this goal requires a more complete experimental information on the aircraft. Recommendations for further development of this research are as follows:

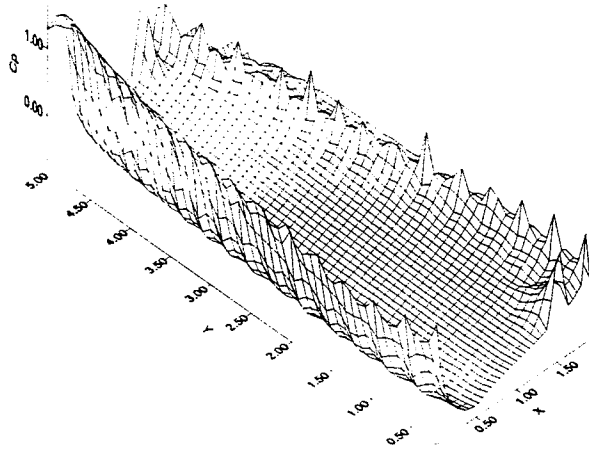
1. In the development of the load models based on wind tunnel testing, the fuselage effects need to be considered in the determination of aircraft aerodynamic characteristics, such as lifting surface lift-curve slopes. More realistic  $C_{m_{owb}}$ ,  $h_o$ , and  $\epsilon$  need to be obtained for more accurate predictions of AOA and  $\eta$  in trimmed flight to be made, and this requires tail-off test data.
2. In the development of the independent model based on lifting line method, more accurate modelling of wing and tailplane geometry and airflow at the tail is necessary.
3. The analysis presented in this thesis applies to a rigid airplane in gliding flight only. For more realistic flight conditions to be simulated, propeller power effects need to be considered.

#### Acknowledgements

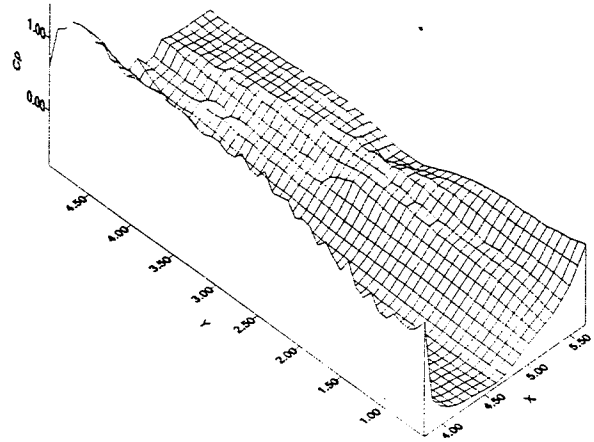
This project was supported by the Department of Aerospace Engineering, RMIT. The author would like to thank Mr. R. Danaher for his guidance. The author would also like to acknowledge AMRL for providing the PC-9 wind tunnel test data.

#### References

- [1] Quick, H.A., "Estimation of Aerodynamic Load Distributions on the F/A-18 Aircraft Using a CFD Panel Code", DSTO Technical Report 0147, 1995.
- [2] Bertin, J.J. and Smith, M.L., "Aerodynamics for Engineers", Prentice Hall, 1989.
- [3] Houghton, E.L. and Carruthers, N.B., "Aerodynamics for Engineering Students", Edward Arnold, 1982.
- [4] Danaher, R., "AE862 - Aircraft Aerodynamic Design", RMIT, 1996.
- [5] "Aircraft Specification - Pilatus PC9", DI(AF) AAP 7212.007-1.
- [6] Taylor, M., "Brassey's World Aircraft & Systems Directory 1996/1997", Brassey's, 1996.

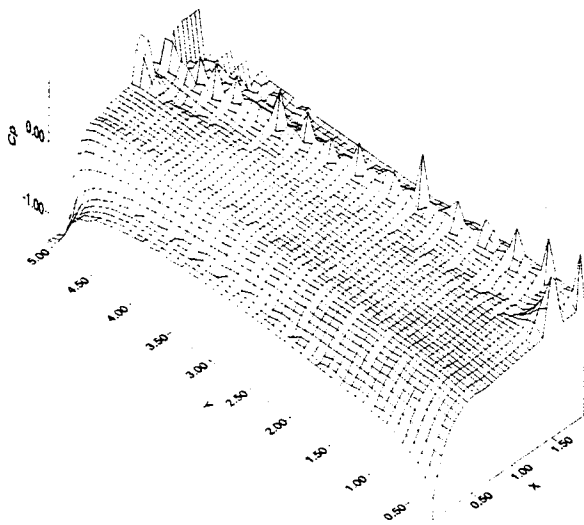


(a) Theoretical

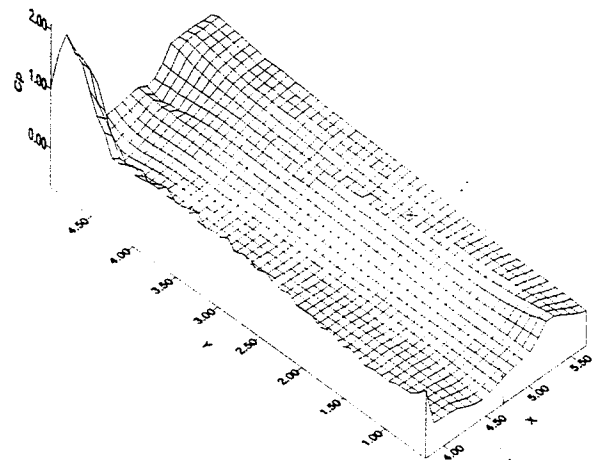


(b) Experimental

Figure 1 Wing upper surface pressure distribution at  $AOA = 0^\circ$  ( $\alpha = 1^\circ$ )

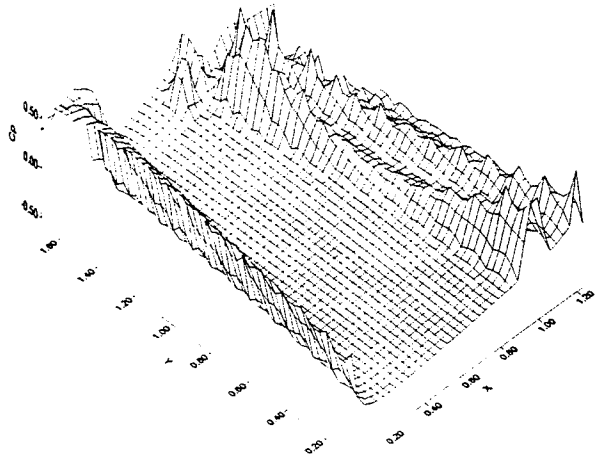


(a) Theoretical

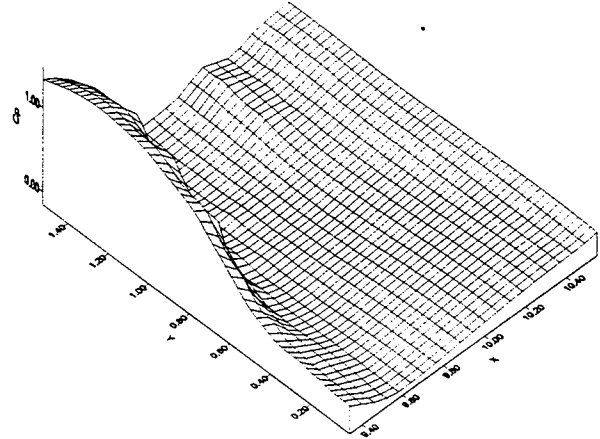


(b) Experimental

Figure 2 Wing lower surface pressure distribution at  $AOA = 0^\circ$  ( $\alpha = 1^\circ$ )

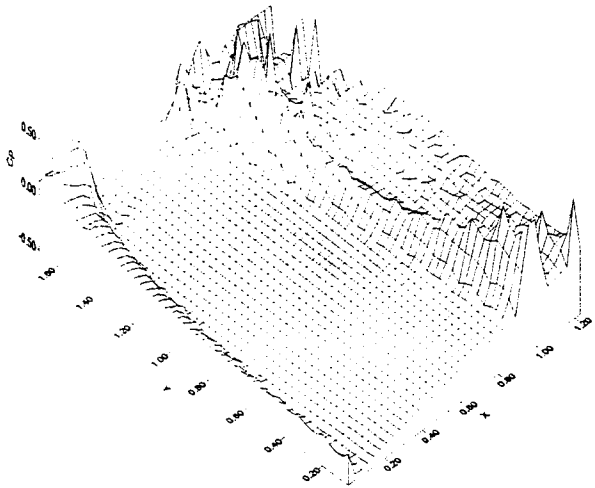


(a) Theoretical

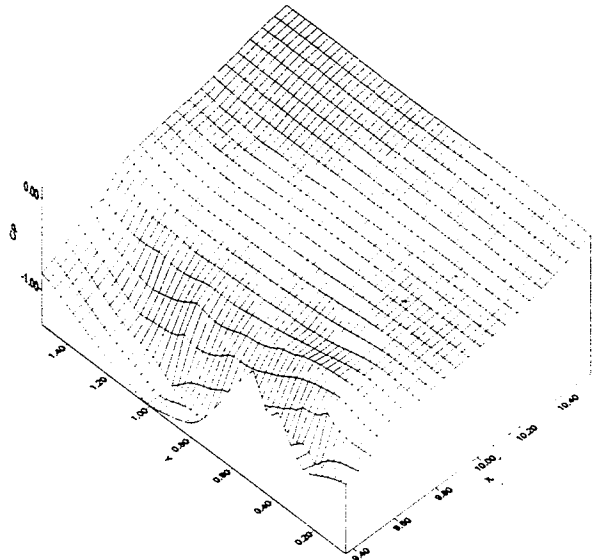


(b) Experimental

Figure 3 Tailplane upper surface pressure distribution at  $AOA = 0^\circ$  &  $\eta = 0^\circ$



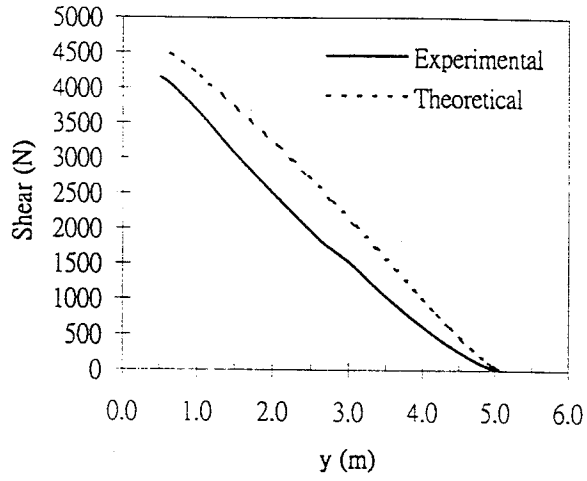
(a) Theoretical



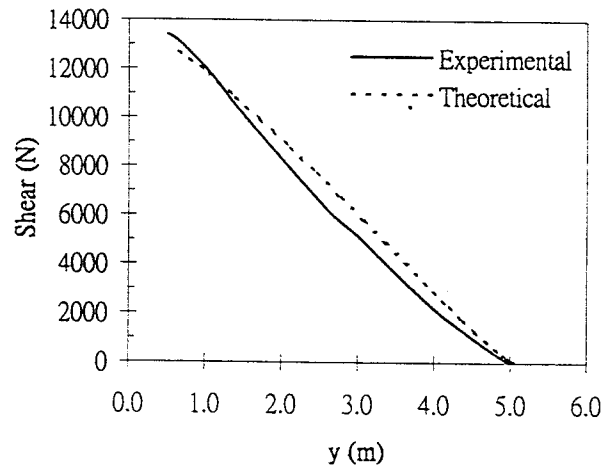
(b) Experimental

Figure 4 Tailplane lower surface pressure distribution at  $AOA = 0^\circ$  &  $\eta = 0^\circ$



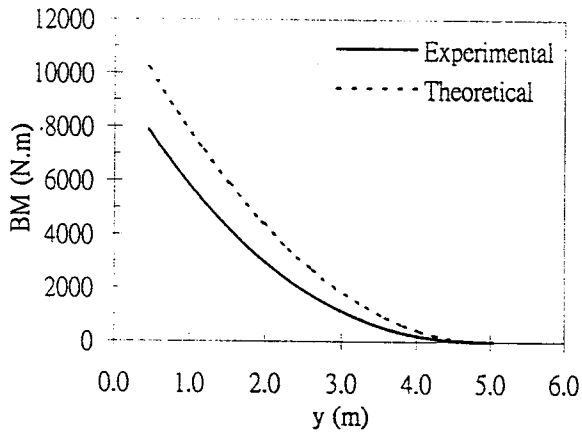


(a) AOA = 0°

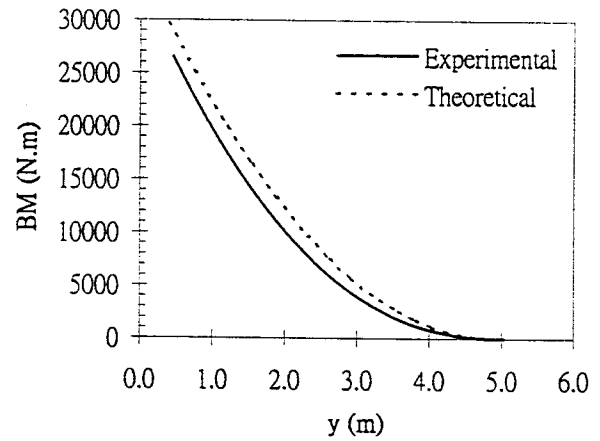


(b) AOA = 8°

Figure 5 Wing shear distribution

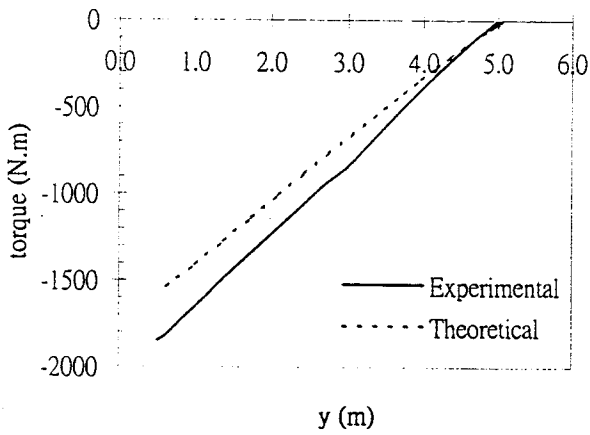


(a) AOA = 0°

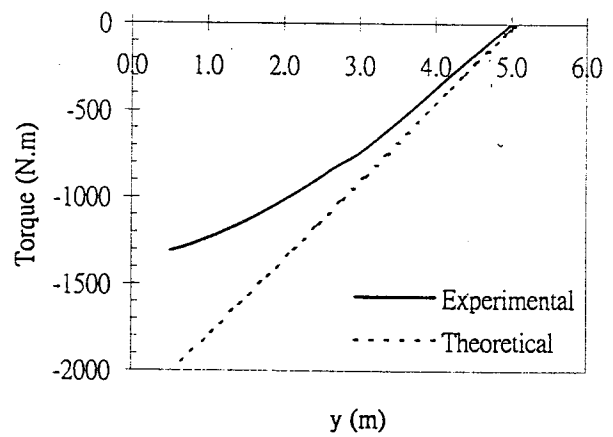


(b) AOA = 8°

Figure 6 Wing bending distribution

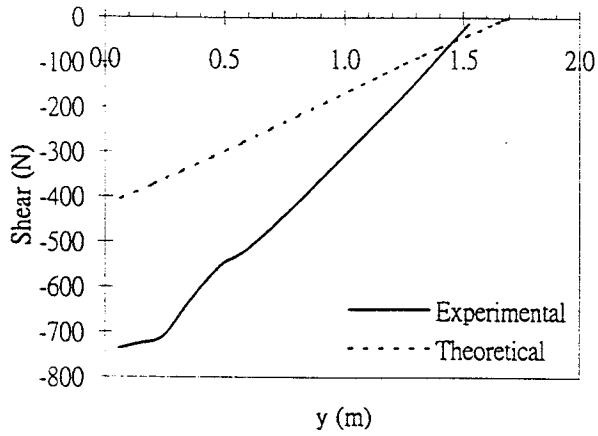


(a) AOA = 0°

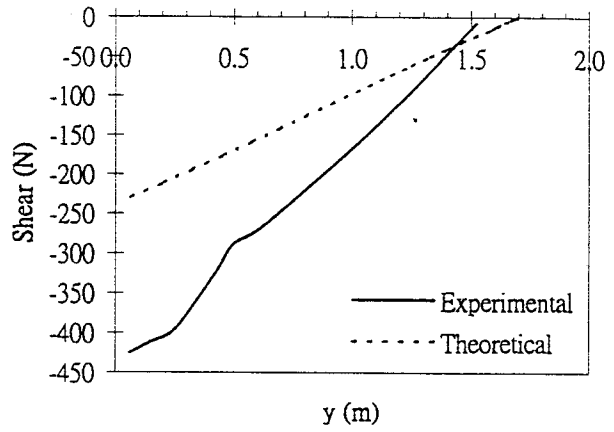


(b) AOA = 8°

Figure 7 Wing torque distribution

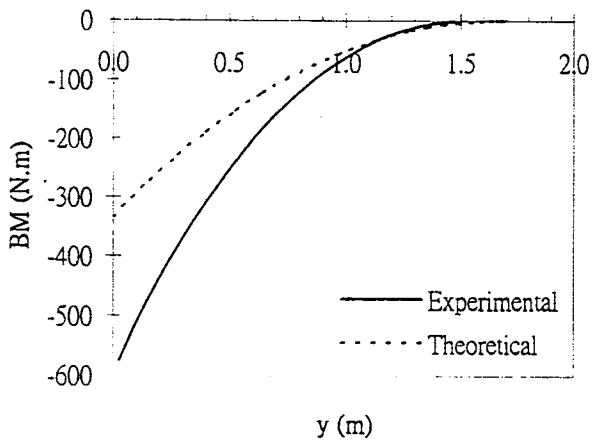


(a) AOA = 0° &  $\eta = 0^\circ$

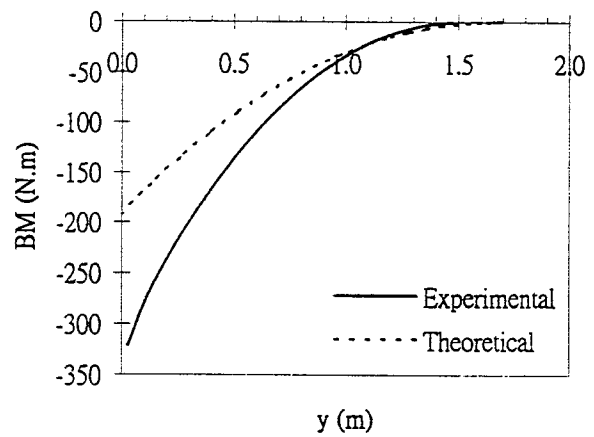


(b) AOA = 8° &  $\eta = -5^\circ$

Figure 8 Tailplane shear distribution

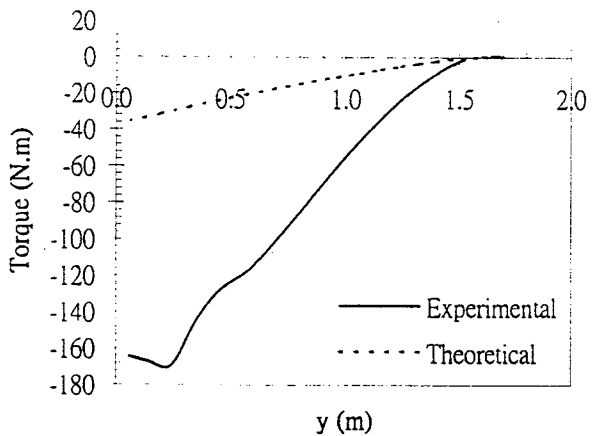


(a) AOA = 0° &  $\eta = 0^\circ$

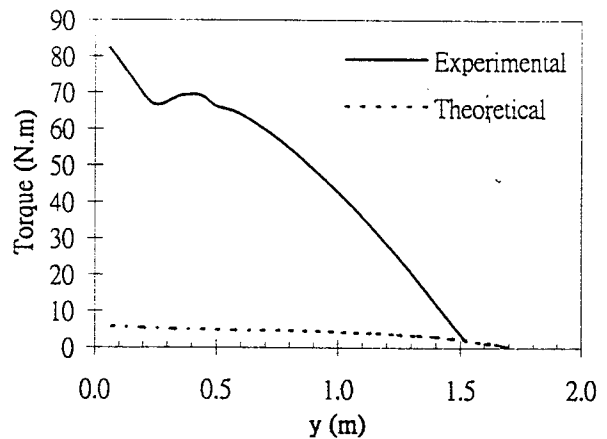


(b) AOA = 8° &  $\eta = -5^\circ$

Figure 9 Tailplane bending distribution



(a) AOA = 0° &  $\eta = 0^\circ$



(b) AOA = 8° &  $\eta = -5^\circ$

Figure 10 Tailplane torque distribution